

Image Processing Method for Intruder Detection around Power Line Towers

Masahisa KANETA[†], Hitoshi KANO[†], Kimiharu KANEMARU[†], Toshio NAGAI[‡]

[†]Hitachi Cable, Ltd.

5-1-1 Hitaka-cho, Hitachi-shi, Ibaraki-ken, 319-14 Japan

[‡]Kansai Electric Power Co., Inc.

11-20 Nakoji, 3-chome, Amagasaki-shi, Hyogo-ken, 661 Japan

ABSTRACT

A method of detecting intruders around power line towers using an image processing technique has been developed. Outdoor images include a variety of factors leading to erroneous image processing, such as rapid changes in brightness, rustling of leaves, mist, rain, and dislocation of power line conductors due to wind. These problems were solved as follows. A change of image is first detected, as an intruder candidate, using a histogram of the difference between a reference image and an observation image. The detected differences are further determined to be an intruder using a circumscribed rectangle, a number, an area, and the center of gravity. The method was field tested and the evaluation confirmed that the successful intruder detection rate was 82%.

1. INTRODUCTION

Monitoring by industrial television (ITV) camera is wide use in many fields, and a desire exists for its processing to be fully automated. Development efforts have been made for outdoor image processing techniques such as automatic navigation and identification of aircraft types. For intruder detection around power line towers, however, there are special considerations. These include some problems such as the detection of unspecified objects, the rustling of leaves, and intrusion by small animals.

In this paper, the effectiveness of this method in eliminating these erroneous factors is shown. That is, a change of image is detected, as an intruder candidate, using a histogram of the differences between the reference image and the observation image. These detected differences are further determined to be an intruder using a circumscribed rectangle, a number, an area, and the center of gravity. First, the problems in outdoor image processing and our basic policies are shown. Then, the algorithms to solve these problems are described. The performance of this method in field tests is also shown.

2. PROBLEMS AND POLICIES

Typical factors in erroneous image processing in intruder detection around power line towers are shown in Table 1.

These problems are solved using the following

Table 1 Typical erroneous factors in image processing in intruder detection around power line towers.

Item	erroneous factor	countermeasure
change in background brightness	<ul style="list-style-type: none"> *rapid change in background brightness (due to cloud movement) *slow change in background brightness (due to shadow movement) 	<ul style="list-style-type: none"> *histogram of the difference image *renewal of reference image
swaying of object due to wind	<ul style="list-style-type: none"> *small rustling of leaves *dislocation of power-line conductors 	<ul style="list-style-type: none"> *smoothing of observation image *circumscribed rectangle
others	<ul style="list-style-type: none"> *mist, rain, flying objects, etc. *birds, small animals *large rustling of leaves 	<ul style="list-style-type: none"> *circumscribed rectangle *position of center of gravity

countermeasures. Against rapid changes in brightness, a histogram of the difference between the reference image and the observation image is used to remove part of a uniform change in brightness. Against slow changes in background brightness, such as the move of shadows, the reference image is renewed in every sequence. Moreover, smoothing filters are used to remove small image changes caused by the rustling of leaves.

The detected portion is further determined by investigating its rough shape using the circumscribed rectangle. From this investigation, false detection from the dislocations of power-line conductors due to wind can be eliminated. Errors caused by mist, rain, and intrusion by small animals are reduced by using the number of detected portions, their areas, and their centers of gravity.

3. IMAGE PROCESSING TECHNIQUE FOR INTRUDER DETECTION

A flow chart of the intruder detection process is shown in Fig. 1. In this figure, the left column is the basic intruder detection process, and the right column is decreasing erroneous factors. Each of these processes is described in this chapter.

3.1 Intruder Detection Process

(1) Basic detection process

The difference in brightness between the reference and observation images is first calculated for each

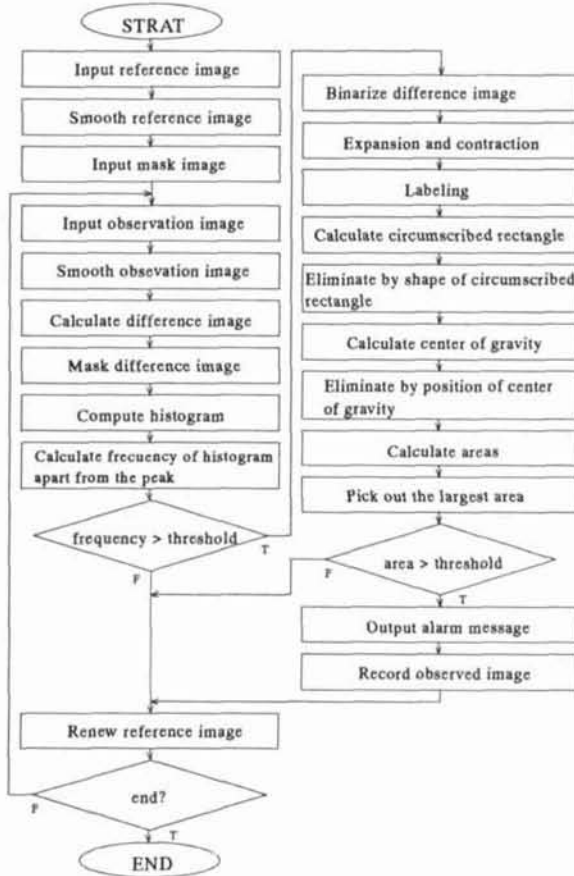


Fig. 1. Flow chart of intruder detection process

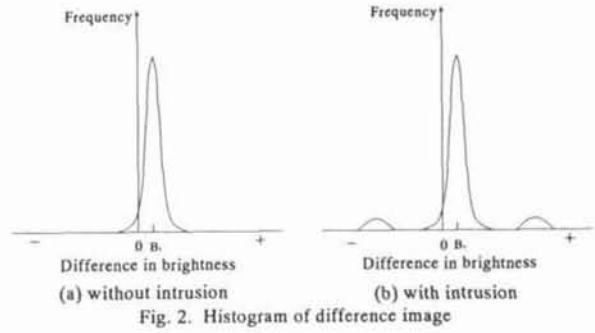
pixel, thus making a difference image. Then the brightness histogram of the difference image is obtained. An example of a histogram of a difference image is shown in Fig. 2. When the observation image does not change with intrusion, the histogram of the difference image is concentrated at around the peak of the brightness difference as shown in Fig. 2(a). When the observation image changes with intrusion, on the other hand, the other high frequency peaks initiate besides the original one as shown in Fig. 2(b). That is, when the other distributions are observed at a distance threshold from the original peak in the histogram, it can be considered that an intruder is detected. The change of lighting condition can not affect the above consideration, since the change only moves the position of the original peak as shown below.

When the brightness of the observation image at time $t=0$ is described by a function $f_0(x,y)$, the brightness of the observation image after t (sec.) can be approximately described by Equation (1) provided that t is small.

$$f_t(x,y) = (1+\epsilon_t) f_0(x,y) + B_t + g_t(x,y) \quad (1)$$

where,

- ϵ_t :coefficient of brightness change proportional to f_0 .
- B_t :uniform change in brightness.



$g_t(x,y)$:change in brightness corresponding to intrusion.

Therefore, the difference Δf_t between f_t and f_0 can be written as Equation (2).

$$\Delta f_t(x,y) = \epsilon_t f_0(x,y) + B_t + g_t(x,y) \quad (2)$$

When the histogram of an image f is expressed by $H[f_0]$, $H[\Delta f_t]$ has two kinds of distribution as shown in Fig. 2(b). One is for the brightness change of background which has the width proportional to ϵ_t around the center B_t , and the other for intrusion $g_t(x,y)$ which has rather broad distribution. These two kinds of distribution can be discriminated when the following requirement satisfies;

$$|\epsilon_t| \ll 1 \quad (3)$$

The condition of t is determined to satisfy Equation (3) by $|\epsilon_t|$ obtained by the experiment.

Figure 3 shows an image taken at a power line tower. Figures 4(a) and (b) are $H[f_0]$ and $H[\Delta f_t]$ of the image shown in Fig. 3, respectively. ϵ_t is considered to be approximately the ratio of the width of $H[\Delta f_t]$ to that of $H[f_0]$, and we get $|\epsilon_t| = 0.34$. Table 2 shows the results of $|\epsilon_t|$ and B_t by the experiment. The results indicate that the average brightness (corresponding to B_t) increases during the first 20 seconds and then decreases due to the move of cloud. $|\epsilon_t|$ changes in proportion to the change of brightness, and $|\epsilon_t| < 0.07$ at $t < 5$ which satisfies the requirement $|\epsilon_t| \ll 1$ described by Equation (3). According to these results, the target interval of reference image of this method is determined to be 5 seconds. Any amount of B_t will not affect this change detection method.

Also, a change in background brightness due to the rustling of leaves is eliminated by applying 5×5 smoothing filters. A mask image is also applied to restrict the observation area so that the brightness changes due to reflection of tower structure, etc. are eliminated.

An example of the change detection process is given in Fig. 5. Figure 5(a) is an observation image, Fig. 5(b) is the image after treating with smoothing filters, Fig. 5(c) is the mask image (black area corresponds to masked area), and Fig. 5(d) is the histogram of difference image. The round mark in Fig. 5(d) is thought to be the part of the change due to an intruder or the dislocation of power line conductors.



Fig. 3. Image of lower part of tower for field test

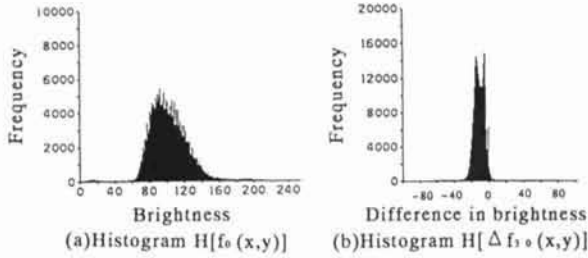


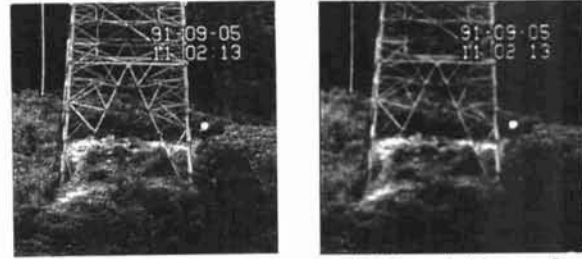
Fig. 4. Histogram of image shown in Fig. 3.

Table 2 Change of B_0 and $|\epsilon_1|$

Time(s)	B_0	$ \epsilon_1 $
1	0	0.043
2	0	0.043
3	0	0.043
4	1	0.065
5	1	0.11
6	2	0.13
7	3	0.13
10	5	0.20
20	14	0.43
30	11	0.34
40	1	0.13
50	5	0.13
60	6	0.17
70	7	0.11

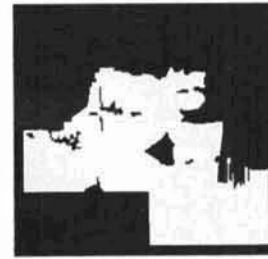
(2) Renewal of reference image

The background brightness will change slowly as time passes. Therefore, differences in the background between the reference and observation images grow gradually. The shadows of trees and structures are examples of the effect. To reduce the difference in the background, the reference image is renewed in every sequence. Specifically, when no intruder is detected, the reference image is replaced by an average of the preceding reference image and the newest observation image. When an intruder is detected, on the other hand, the reference image is replaced by an average of the reference and observation images exclusive of the detected region.

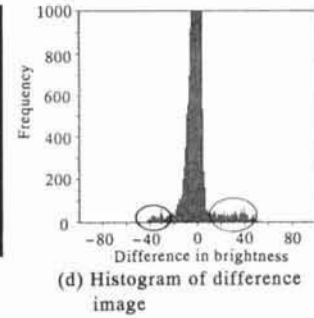


(a) Observation image

(b) Smoothed image of observation image



(c) Mask image



(d) Histogram of difference image

Fig. 5. Example of change detection process

3.2 Procedure for Decreasing Erroneous Factors

It was confirmed by experiments that the basic procedure mentioned above invites false detection due to mist, rain and dislocation of power-line conductors. Therefore, the detected portion is further examined by investigating its rough shape using a circumscribed rectangle. This procedure is shown in the right column of Fig. 1.

First, the difference image is binary coded, and expanded and contracted to fill lost holes, and the connected components are assigned labels. The centers of gravity, areas and the circumscribed rectangle are calculated for each label. Next, the connected components longer or larger than the predetermined threshold values are eliminated. The labels with centers of gravity located in unexpected regions are also eliminated. Next, the largest area of connected components is obtained, and when this area is greater than the threshold value, an intruder is considered to be detected. The process initiates an alarm message and records the observed image. When the largest area of connected components is smaller than the threshold value, the process considers that no intrusion has occurred and renews the reference image. This is the procedure for decreasing erroneous factors.

4. EVALUATION OF PROCEDURE

To confirm the capability of this procedure, field testing was conducted at a power line tower. An example of the ITV image in the field test is shown in Fig. 3. The distance from the ITV camera to the tower was about 350 meters. The weather condition was changing and rather heavy with wind and mist.

The image processor used in the field test has 512×480 pixels each having 256 brightness levels,

Table 3 Characteristic features of object

Feature	area	circumscribed rectangle			center of gravity	
		l_x	l_y	l_x/l_y	x	y
power-line conductor 1	$100 < A$	$40 < l_x < 50$	$50 < l_y < 220$			$y < 150$
power-line conductor 2	$100 < A$	$150 < l_x < 250$	$250 < l_y < 480$			
small animals, etc.	$A < 200$			< 1		
mist	$2000 < A$					
man	$50 < A < 500$			> 1		

and performs filtering, labeling, generating histogram, expansion and contraction by hardware.

First, characteristic features of the objects in the observation image are summarized in Table 3. In the table, A indicates the area of connected components, (l_x, l_y) indicates the lengths of sides of circumscribed rectangle, and (x, y) indicates the position of center of gravity. Small animals or mist cannot be discriminated from intruders only by area A. By using circumscribed rectangle (l_x, l_y) in addition to area A, however, an intruder (man) can be discriminated from small animals or mist by the following logical expression;

$$(200 < A < 500) \vee (50 < A < 200) \wedge (l_x < l_y) \quad (4)$$

Where, \vee :logical sum, \wedge :logical product. Also, dislocation of power line conductors cannot be discriminated from intruders only by area A. By introducing the position of center of gravity, it can be detected by the following expression;

$$(A < 50) \wedge (l_x < 40) \wedge (l_y < 50) \wedge (y > 150) \quad (5)$$

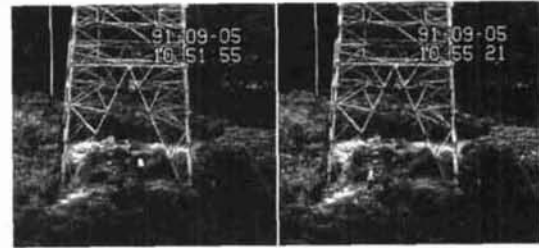
And finally, the detection of an intruder exclusively can be made by the following logical condition;

$$\{(200 < A < 500) \vee (50 < A < 200) \wedge (l_x < l_y)\} \wedge (l_x < 40) \wedge (l_y < 50) \wedge (y > 150) \quad (6)$$

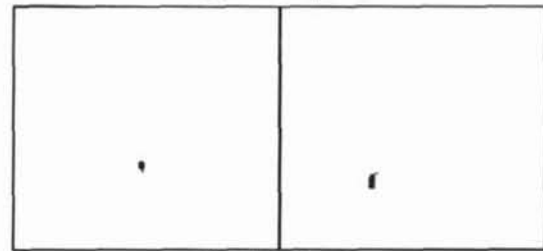
The evaluation was made with these conditions. The execution time of the basic process is about 3 seconds. When no intruder is detected, the execution time of the decreasing erroneous factors is also about 3 seconds. When an intruder is detected, on the other hand, the time for decreasing erroneous factors is about 6 seconds. Test intrusions were made 44 times in 5 hours, and this procedure detected the intruders 36 times (percentage of detection is 82%). The ratio of false detection to the number of total detection was 6% as shown in Table 4. The detected image is shown in Fig. 6. From these results of field testing, it was confirmed that the method can effectively eliminate various erroneous factors such as brightness change in background, rustling of leaves, dislocation of power line conductors, mist and rain, and perform accurate intruder detection. As described above, good results

Table 4 Results of field testing

number processed	total detection n_t	successful detection n_s	false detection n_f	the false detection rate n_f/n_t
2919	134	126	8	6%



(a) ITV image



(b) Detected part

Fig. 6. Example of ITV image and detected part in field test

were obtained even in an outdoor environment with many erroneous factors.

5. CONCLUSIONS

In this paper, the problems in detecting intruders around power line towers using image processing were listed, and countermeasures were proposed. An intruder detection method was developed and evaluated in field tests. It was confirmed that the rate of successful intruder detections was 82%. Based on these results, further improvement in performance is planned using domain specific knowledge of the target image.

ACKNOWLEDGMENTS

The authors wish to thank Dr. Naokazu Yokoya of the Electrotechnical Laboratory for his guidance and discussions in carrying out this research. Also, we wish to thank Kyuichi Sasahara and Kentarou Tsuru of Hitachi Cable, Ltd., for their cooperation.

REFERENCES

- [1] Heitou Zen et al.: "Analysis of a Road Image as Seen from a Vehicle", *Trans. the Institute of Electronics, Information and Communication Engineers of Japan, Vol. J71-D, No.9, pp.1709-1717, 1988.*
- [2] Yasuo Kudo: "Traffic Flow Measurement System Using Image Processing", *Trans. the Institute of Electronics, Information and Communication Engineers of Japan, Vol. J68-D, No.3, pp.308-315, 1985.*